PAPER

Check for updates

Comparison of electro-oxidation coupled with UV irradiation (UV/EO) *versus* conventional oxidation processes (UV irradiation, chlorination, electro-oxidation, and UV/chlorine) for atenolol removal: role of operating parameters, energy performance, and toxicity

Pannika Duangkaew and Songkeart Phattarapattamawong [ID] *

In this study, electro-oxidation combined with UV irradiation (UV/EO) was used for atenolol (ATL) removal, and the results were compared with those of electro-oxidation (EO), UV irradiation, UV/chlorine, and chlorination. In addition, effects of current density (CD), UV intensity, electric potential, electrolyte (NaCl) concentration, ATL concentration, pH, and free radicals were studied. The UV/EO process was the most effective for ATL removal, followed by UV/chlorine, EO, chlorination, and UV irradiation. The ATL degradation was described by a pseudo-first-order rate model, and the observed rate constant (k') for UV/EO exhibited a direct proportionality to CD, NaCl concentration, and UV intensity. In contrast, the results were opposite for pH and ATL concentration. A change in the electric potential did not affect the UV/EO efficiency. The energy consumption of the UV/EO process exhibited an inverse proportionality to the k' value. $^{\bullet}$OH played the major role in ATL removal, while the role of RCS was minor. The kinetic degradation of ATL by $^{\bullet}$Cl ($k_{Cl^{\bullet}}$) was 1.55×10^{11} M^{-1} s^{-1}. Intermediate products formed during ATL oxidation exhibited higher toxicity than the parent compound. This finding highlights the potential risks associated with the formation of highly toxic byproducts. Therefore, it is necessary to optimize the design and operating parameters of the UV/EO system to prevent the formation and accumulation of harmful intermediates.

1. Introduction

Pharmaceutical and personal care products (PPCPs) are active organic compounds that often pollute water resources, causing adverse effects on the ecosystem. Due to their high stability and limited uptake by the body, PPCPs are released through wastewater into the environment.[1] Pharmaceutical pollutants are difficult to remove by conventional wastewater treatment because they are present in trace amounts and some of them can resist biodegradation. Atenolol (ATL), a beta-blocker drug used to treat heart and vascular diseases, is a non-biodegradable compound with long persistence in the environment, and 50–85% of consumed ATL is excreted through urine.[2] The ATL structure ($C_{14}H_{22}N_2O_3$) includes a phenyl ring with an acetamide group on one side and an ether-linked hydroxypropanolamine chain on the other side (SI Fig. 1). ATL exhibits limited direct absorption in the visible light region. As a result, the removal efficiency under visible light is minor, with
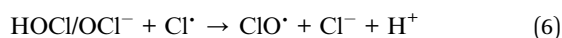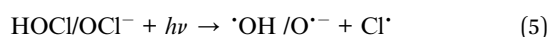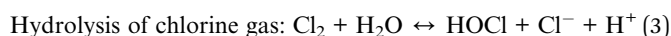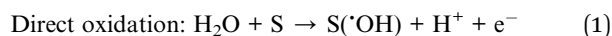
about 15% degradation observed after 120 min of exposure.[3,4] ATL has been found in the environment at a concentration of 0.040–122 μg L^{-1}.[5] It has been shown to inhibit the growth of human embryonic cells and exhibit toxicity toward freshwater species.[6] Among 3466 chemical compounds found in the environment, ATL is one of 36 PPCPs identified as a priority in the global risk ranking list.[7] In addition, the toxicity of products derived from ATL degradation is unknown.

In general, water treatment involves either chlorination or UV irradiation as the final process. However, chlorination and UV irradiation have been reported to be ineffective for ATL removal.[8,9] Moreover, chlorination requires careful chemical management, as transportation, storage, and handling of chlorine pose significant safety concerns. In this context, the generation of chlorine *in situ* offers an attractive alternative by reducing safety risks and providing operational flexibility. Electro-oxidation (EO) simultaneously generates free active chlorine (FAC) and hydroxyl radicals ($^{\bullet}$OH) on the electrode surface (S) (eqn (1)–(4)).[10] Electro-oxidation combined with UV irradiation (UV/EO) is considered to be a novel advanced oxidation process (AOP) because it enhances the generation of

Department of Environmental Engineering, King Mongkut's University of Technology Thonburi, Thailand. E-mail: songkeart.pha@kmutt.ac.th; Tel: +662-470-9163

diverse reactive radicals. Decomposition of FAC (HOCl/OCl⁻) by UV photolysis leads to the formation of ˙OH and various reactive chlorine species (RCS) (eqn (5)–(7)).[11–13] This approach not only overcomes the limitations of conventional oxidation processes but also enhances oxidative capacity, making it a promising option for efficient ATL removal. The UV/EO process can be applied over a broad pH range,[14,15] whereas the Fenton process, a conventional AOP, is predominantly used for treating acidic wastewater due to the preferred oxidation state of iron under acidic conditions.[16,17] In the Fenton reaction, ferrous ions react with hydrogen peroxide to generate ˙OH. Recent studies have developed visible-light-driven photocatalysts to enhance the efficiency and practical application of the process.[18,19] However, UV-based AOPs are readily implemented in water purification because the interference from suspended solids or turbidity is relatively minor compared with that in wastewater treatment. The oxidation potentials of ˙OH, Cl˙, $Cl_2{}^{˙-}$, and OCl˙ are 2.8, 2.43, 2.13, and 1.39 eV, respectively.[20,21] These active radicals are powerful oxidants for the removal of recalcitrant pollutants.[22] The ˙OH is a strong and non-selective oxidant, while RCS are more selective for unsaturated and aromatic compounds.[23] The predominant reactant significantly influences the reaction efficiency and the structural characteristics of the oxidation byproducts, thereby affecting their toxicity. Previous research found that, rather than ˙OH, RCS enhanced trimethoprim degradation rate to 87%, and played a major role in the removal process.[24] RCS can interact with organic compounds through chlorine addition, electron transfer, and H-abstraction.[25,26] These reactions contribute to the formation of disinfection byproducts, which include compounds with potential carcinogenic and mutagenic properties.[27,28] Although the kinetic degradation rate of ATL by ˙OH has been reported,[29,30] studies on the rate of ATL degradation by RCS are limited, and further research is needed to elucidate the nature of the active radicals.

$$\text{Direct oxidation: } H_2O + S \rightarrow S(˙OH) + H^+ + e^- \quad (1)$$

$$\text{Anodic reaction chlorine: } 2Cl^- \rightarrow Cl_2 + 2e^- \quad (2)$$

$$\text{Hydrolysis of chlorine gas: } Cl_2 + H_2O \leftrightarrow HOCl + Cl^- + H^+ \quad (3)$$

$$\text{Equilibrium at pH 7.5: } HOCl \leftrightarrow OCl^- + H^+ \quad (4)$$

$$HOCl/OCl^- + h\nu \rightarrow ˙OH /O^{˙-} + Cl˙ \quad (5)$$

$$HOCl/OCl^- + Cl˙ \rightarrow ClO˙ + Cl^- + H^+ \quad (6)$$

$$Cl^- + Cl˙ \rightarrow Cl_2{}^{˙-} \quad (7)$$

The formation of free radicals depends on operational and environmental factors, such as current density (CD), electric potential, electrolytic concentration, pollutant concentration, and pH.[13,31,32] The electrical current decomposes electrolytes such as chloride to form chlorine gas on the surface. The chlorine is dissolved and hydrolyzed to hypochlorous acid (HOCl), which further dissociates to hypochlorite (OCl⁻). The amount of chlorine depends on the CD and the electrolyte concentration.[33] However, information on the practical aspects

of this process is currently limited. A key question to explore is whether substance removal is primarily governed by electric potential or CD. Investigating the relative contributions of these factors could provide valuable insights into optimizing removal efficiency in various treatment processes. This knowledge is also useful for the development and operation of UV/EO processes.

The aim of this study was to remove ATL using the UV/EO process and to compare the outcome with those achieved by using electrooxidation (EO), UV irradiation, UV/chlorine, and chlorination processes. In addition, the influence of various operating factors (*i.e.*, current density (CD), electric potential, electrolytic concentration, ATL concentration, pH, and free radicals) on the effectiveness and energy performance was studied. The effect of operating factors on the kinetic degradation of ATL by the UV/EO process was also revealed. Lastly, the microbial toxicity of the treated water was tested. The findings show the potential of the UV/EO process for removing pharmaceutical compounds while minimizing energy demand.

2. Materials and methods

2.1. Materials

ATL (purity >98%) was purchased from Sigma-Aldrich. The electrolyte was sodium chloride (purity >99%) purchased from Carlo-Erba. Sodium hypochlorite solution (concentration >7%) was laboratory grade. Ultrapure water (UPW) was generated from an Arium® Pro DI/UV water filter (Sartorius, Germany).

The reactor was housed in an opaque, rectangular wooden box with dimensions of 41 × 42 × 40 cm (W × L × H). Three low-pressure UV-C lamps (Philips, 6 W, 20 mm inner diameter and 355 mm long) were mounted within a quartz glass tube on the ceiling of the enclosure (SI Fig. 2). The UV lamp was warmed for 30 min before starting the experiment. The UV intensities for one, two, and three UV lamps were 0.281, 0.506, and 0.681 mW cm⁻², respectively, as determined with an actinometer and the iodide/iodate method.[34] The electrodes were constructed with BDD (anode) and Ti (cathode). The space and surface area of the electrodes were 3.5 cm and 28 cm², respectively.

2.2. Experimental procedure

Samples (400 mL) were prepared in UPW in a glass beaker and placed onto a magnetic stirrer. The pH was controlled with a phosphate buffer solution at pH 6, pH 7, and pH 8 (10 mM). The electrolyte was prepared in a phosphate buffer solution by adding sodium chloride (NaCl) at 300, 500, and 1000 mg L⁻¹. A chlorine concentration of 24 mg L⁻¹ was used for the chlorination process. This chlorine concentration was the maximum chlorine residual formed in the EO and UV/EO processes. The ATL concentration was 20 ± 0.5 μg L⁻¹. A power supply (LW-3010KDS, LONG WEI) was used to deliver currents at 0.07, 0.14, and 0.28 A to achieve CDs of 2.5, 5, and 10 mA cm⁻², respectively. The electric potentials were recorded at 7 ± 1, 10 ± 1, and 12 ± 1 voltages, respectively. The experiment was performed at 25 °C in batch mode for 120 min. To study the effect of free radicals (˙OH and RCS), *para*-chlorobenzoic acid (*p*CBA)

and benzoic acid (BA) were used. pCBA was selected as a probe to differentiate the role of ˙OH, instead of nitrobenzene. Although nitrobenzene is a scavenger of ˙OH with negligible reaction with Cl˙,[35] the high molar extinction coefficient of nitrobenzene at 254 nm (5858 M^{-1} cm^{-1}) can interfere the UV photolysis and UV-based advanced oxidation processes.[36] On the other hand, UV photolysis of pCBA at 254 nm is negligible,[37] indicating a low molar extinction coefficient and quantum yield. BA has been used as a probe for various free radicals (*i.e.*, ˙OH and Cl˙).[38,39] $Na_2S_2O_3$ was used as a quenching agent of free chlorine. Each experiment was performed in triplicate.

2.3. Analytical methods

The ATL concentration was determined by high-performance liquid chromatography (HPLC, Waters e2695). A C18 column (Vertisep™ AQS, 4.6 mm × 150 mm, 5 μm) was used to separate the compounds in the sample. The mobile phase solution was prepared by mixing methanol and phosphate buffer solutions at pH 2.4 in a ratio of 25 : 75, and a flow rate of 1 mL min^{-1} was used. The sample injection volume was 100 μL. A UV detector at 254 nm was used to quantify the ATL, and the column temperature was 30 °C. The limit of detection (LOD) of ATL was 0.5 μg L^{-1}. Nitrobenzene (NB) and benzoic acid (BA) were analyzed using HPLC (Nexera Series, Shimadzu) with a C18 column (Vertisep™ AQS, 4.6 mm × 150 mm, 5 μm). The mobile phase consisted of a methanol and phosphoric acid mixture (pH 2.11) in a 45 : 55 ratio. The analysis was conducted at a flow rate of 1 mL min^{-1} with an injection volume of 10 μL, using a UV detector set at 227 nm and a column temperature of 30 °C. The free active chlorine (FAC) was determined by using the *N,N*-diethyl-*p*-phenylenediamine (DPD) method. pH was measured with a pH meter (portable S2, Mettler Toledo).

Free radical concentrations were calculated using eqn (8) and (9).

$$\frac{d[pCBA]}{dt} = k_{pCBA-\cdot OH}[\cdot OH][pCBA] \tag{8}$$

$$\frac{d[BA]}{dt} = (k_{BA-\cdot OH}[\cdot OH] + k_{BA-Cl\cdot}[Cl\cdot])[BA] \tag{9}$$

where $k_{pCBA-\cdot OH}$, $k_{BA-\cdot OH}$, and $k_{BA-Cl\cdot}$ are second-order reaction rate constants for pCBA with ˙OH (5×10^9 M^{-1} s^{-1}), BA with ˙OH (5.9×10^9 M^{-1} s^{-1}), and BA with Cl˙ (1.8×10^{10} M^{-1} s^{-1}), respectively.[35,39,40] [˙OH] and [Cl˙] are the concentrations of ˙OH and Cl˙, respectively.

The specific energy consumption of UV/EO for 90% ATL removal (E, kWh m^{-3}) can be estimated by using eqn (10).[41,42]

$$E = \frac{UIt_{90\%}}{1000V} + \frac{Pt_{90\%}}{1000V} \tag{10}$$

where I is the applied current (A), U is the applied voltage (V), $t_{90\%}$ is the time at 90% removal (h), P is the power imparted to the water (W), and V is the solution volume (m^3).

Bacterial toxicity was tested with *Bacillus cereus* (*B. cereus*), a Gram-positive rod-shaped bacterium. The method was modified slightly from a previous study.[43] *B. cereus* was inoculated in culture medium (K_2HPO_4 2.64 g L^{-1}, KH_2PO_4 1.64 g L^{-1},

glucose 0.2 g L^{-1}, and acetate 0.2 g L^{-1}, nutrient broth 1.6 g L^{-1}) for 18 h before storage in a refrigerator. Resazurin (0.5 mg L^{-1}) was used as an inhibiting reagent to assess metabolic activity and cell viability. Mixtures of samples and cell cultures were incubated for 20 min before adding 1 mL of resazurin reagent. Bacterial growth changed the resazurin color from blue to pink. The color development was maintained for 20 min. $HgCl_2$ solution (50 μL, 10 mg mL^{-1}) was used to inhibit bacterial growth. The toxicity was determined by measuring the absorption at 610 nm with a spectrophotometer. The inhibition percentage was calculated from eqn (11). The cell control sample (positive control) was a mixture of cells with culture medium and UPW, while the reagent control (negative control) sample was similar to the cell control sample without the addition of cells.

$$\text{Inhibition}(\%) = \frac{\text{sample} - \text{cell control}}{\text{reagent control} - \text{cell control}} \tag{11}$$

3. Results and discussion

3.1. Comparative ATL removals

Chlorination and UV irradiation for 120 min removed 30% and 20% of ATL, respectively (Fig. 1). The partial ATL removal by both methods, which was consistent with previous studies, was attributed to the low extinction coefficient ($\varepsilon_{254} = 462.5$ M^{-1} cm^{-1}) and quantum yield ($\Phi_{254} = 0.002$ M × Einstein^{-1}) for UV photolysis,[9] and to the lower reactivity towards chlorine.[8,30] The ineffective UV photolysis in ATL degradation resulted in an estimated time required for complete ATL removal of 24.6 h (1475 min), rendering the process impractical for implementation. The EO and UV/EO processes effectively reduced the ATL concentration to below the level of detection at 120 min and 50 min, respectively. The EO process generated ˙OH on the electrode surface[10] and FAC (HOCl/OCl$^-$) in the electrolyte to remove the target pollutants.[12] Comparison of the EO and chlorination processes at the same chlorine concentration (24 mg L^{-1}) indicated that the EO process removed more
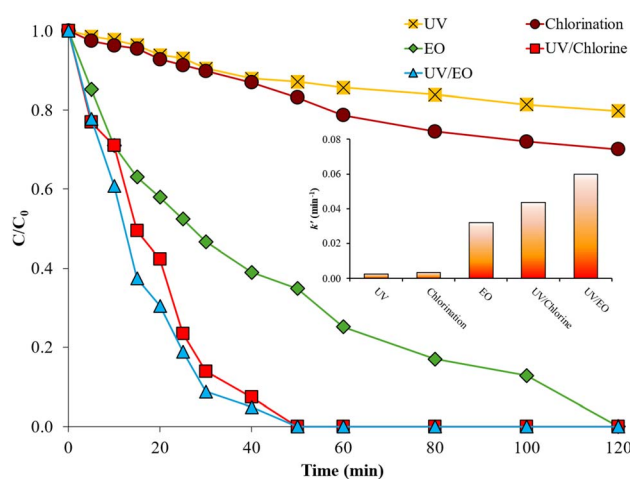

Fig. 1 Removal of ATL by chlorination, UV irradiation, EO, UV/chlorine, and UV/EO (pH 7, NaCl 500 mg L^{-1}, 1 UV lamp, CD 5 mA cm^{-2}, $n = 3$).

ATL, due to the generation of $^{\bullet}OH$ in the system. The oxidation potentials of HOCl and OCl^{-} are lower than that of $^{\bullet}OH$, with values of 1.49 and 0.90 eV, respectively.[44] The UV/EO and UV/chlorine processes generate $^{\bullet}OH$ and RCS *via* UV photolysis of FAC (HOCl/OCl^{-}).[11,38] The mechanism of formation of $^{\bullet}OH$ and RCS in the UV/EO and UV/chlorine processes can be described by eqn (5)–(7).[11–13] Briefly, the O–Cl bond of FAC is cleaved homolytically, producing either $^{\bullet}OH$ from HOCl or oxygen-centered radicals (O$^{\bullet-}$) from OCl^{-}, along with Cl$^{\bullet}$. Hypochlorite (ClO$^{\bullet}$) or dichloride (Cl$_2^{\bullet-}$) radicals can form during the reaction of Cl$^{\bullet}$ with FAC or chloride ion, respectively. Regarding reactive oxygen species, the superoxide radical (O$_2^{\bullet-}$) and hydrogen peroxide (H$_2$O$_2$) are mild to weak oxidants, compared to $^{\bullet}OH$. The contribution of O$_2^{\bullet-}$ and H$_2$O$_2$ to ATL degradation can be negligible due to their low redox potentials.[45,46] However, the presence of O$_2^{\bullet-}$ promoted the H$_2$O$_2$ generation, which may further lead to the formation of $^{\bullet}OH$. Singlet oxygen (^{1}O$_2$) can attack the aromatic moiety of ATL by hydroxylation or cleavage ($k = 7.0 \times 10^5$ M^{-1} s^{-1}).[47] However, the ^{1}O$_2$ oxidation of ATL could be minor because its formation by UV photooxidation of natural organic matter (DOM$^{\bullet} \downarrow {}^1O_2$) can be negligible due to the presence of lower amounts of natural organic matter in our study. In addition, the quantum yield of ^{1}O$_2$ is typically 0.007–0.064,[48] resulting in ^{1}O$_2$ concentrations that are often on the order of 10^{-14}–10^{-13} M.[49,50] $^{\bullet}OH$ is a strong and non-selective oxidant with an oxidation potential of 2.8 eV, while the oxidation potentials of Cl$^{\bullet}$, Cl$_2^{\bullet-}$ and ClO$^{\bullet}$ are 2.43, 2.13, and 1.39 eV, respectively.[20,21] The presence of highly reactive free radicals contributed to the enhanced effectiveness of the UV/EO and UV/chlorine processes, compared to the EO process. Among various treatments, the UV/EO process was the most effective ATL removal process.

The ATL degradation could be described by a pseudo-first-order reaction using the initial reaction-rate method. The determination coefficient (R^2) was over 0.97 (SI Fig. 3). The pseudo-first-order reaction rate constants (k') for UV irradiation and chlorination exhibited comparable values of 0.0025 and 0.0035 min^{-1}, respectively. The EO process enhanced the ATL degradation rate, resulting in a k' value of 0.0319 min^{-1}. The k' values of the UV/chlorine and UV/EO processes were 0.0437 and 0.0599 min^{-1}, respectively. The observed k' value for the UV/EO process exceeded the summation of the individual k' values obtained from the UV irradiation and EO processes. This finding suggested the presence of a synergistic effect in the ATL removal, likely due to the enhanced generation of reactive oxidants and improved degradation pathways when both processes are applied simultaneously. The k' values determined using the initial rate method exhibited slight deviations from the overall degradation rate of ATL obtained through holistic removal (SI Fig. 3). Although an oxidation byproduct was presumably more resistant, the formation of free radicals (*i.e.*, $^{\bullet}OH$ and RCS) was sufficient to sustain the reaction rate.

3.2. Effect of operating parameters on UV/EO

3.2.1. UV intensity.
The UV intensity directly depended on the number of UV lamps. The UV intensities for 1, 2, and 3 UV lamps were 0.2809, 0.5059, and 0.6914 mW cm^{-2}, respectively. Higher UV intensities induced greater ATL removal rates; thus, ATL could not be detected at 45, 25, and 20 min after irradiation with 1, 2, and 3 UV lamps, respectively (Fig. 2a). Because FAC was cleaved and converted into $^{\bullet}OH$ and RCS by UV photolysis, higher UV intensity enhanced the formation of free radicals, resulting in faster removal rates.[51] The k' values for 1, 2, and 3 UV lamps were 0.0599, 0.0917 and 0.1602 min^{-1}, respectively (SI Fig. 4). The k' value was directly proportional to UV intensity, with the corresponding value of 0.2407.

3.2.2. Current density (CD).
An increase in the CD clearly enhanced the ATL removal (Fig. 2b). With a CD of 2.5 mA cm^{-2}, more than 80 min was required for complete ATL removal. Increasing the CD to 5 and 10 mA cm^{-2} reduced the required removal time to 50 and 25 minutes, respectively. Higher CD promoted FAC formation, as evidenced by the FAC concentrations at 120 min of 13, 23.8, and 28 mg L^{-1} for CDs of 2.5, 5, and 10 mA cm^{-2}, respectively. The increase in electrical current supplied more electrons at the anode, promoting water oxidation and resulting in increased formation of chlorine and $^{\bullet}OH$. The applied currents were 0.07 ± 0.01, 0.14 ± 0.01, and 0.28 ± 0.02 A, respectively. These stable currents provided CDs of 2.5 ± 0.5, 5.0 ± 0.3, and 10.0 ± 0.7 mA cm^{-2}, respectively (SI Fig. 5). FAC formation was directly proportional to the CD, with the corresponding value of 1.8343 ($R^2 = 0.8194$). The increase in the rate of ATL removal was demonstrated by the higher k' values (SI Fig. 6). The k' values for CDs of 2.5, 5, and 10 mA cm^{-2} were 0.0427, 0.0599, and 0.1309 min^{-1}, respectively, demonstrating a direct proportionality between the reaction efficiency and the CD. The correlation between the CD and the k' values in this study was consistent with our recent findings, which demonstrated that the k' values for pesticide degradation increased with higher CD. Specifically, the k' values were 0.0374, 0.0450, and 0.0503 min^{-1} at CDs of 5, 10, and 20 mA cm^{-2}, respectively.[52] The k' values increased by 0.0121 per unit increase in CD. The k' value for a CD of 10 mA cm^{-2} was two and three times higher than those observed at CDs of 5 and 2.5 mA cm^{-2}, respectively. The formation of $^{\bullet}OH$ and RCS depends on the UV fluence and the initial substrate concentration (*i.e.*, FAC). Increases in CD, which enhanced FAC formation, enhanced the anodic oxidation and the formation of $^{\bullet}OH$ and RCS in the bulk phase *via* UV photolysis of FAC. Therefore, FAC served as an indirect indicator of the UV/EO process potential, particularly for bulk-phase radical generation under UV irradiation.

3.2.3. NaCl concentration.
The NaCl solution served as the electrolyte, providing ions to carry the electric current during the UV/EO process at a CD of 5 mA cm^{-2} and pH 7 (controlled by a phosphate buffer solution). An increase in NaCl concentration could promote higher conductivity and lower resistance, allowing for better charge transfer and faster reaction rates.[12,53,54] However, a slight increase in the NaCl concentration from 300 to 500 mg L^{-1} led to a marginal enhancement in ATL removal (Fig. 2c). At NaCl concentrations of 300, 500, and 1000 mg L^{-1}, complete ATL removal was achieved within 50, 50, and 30 min, respectively. The minimal impact on ATL removal rates at lower levels of electrolyte concentration was evidenced by the gradual increase in k' values. The k' values at NaCl
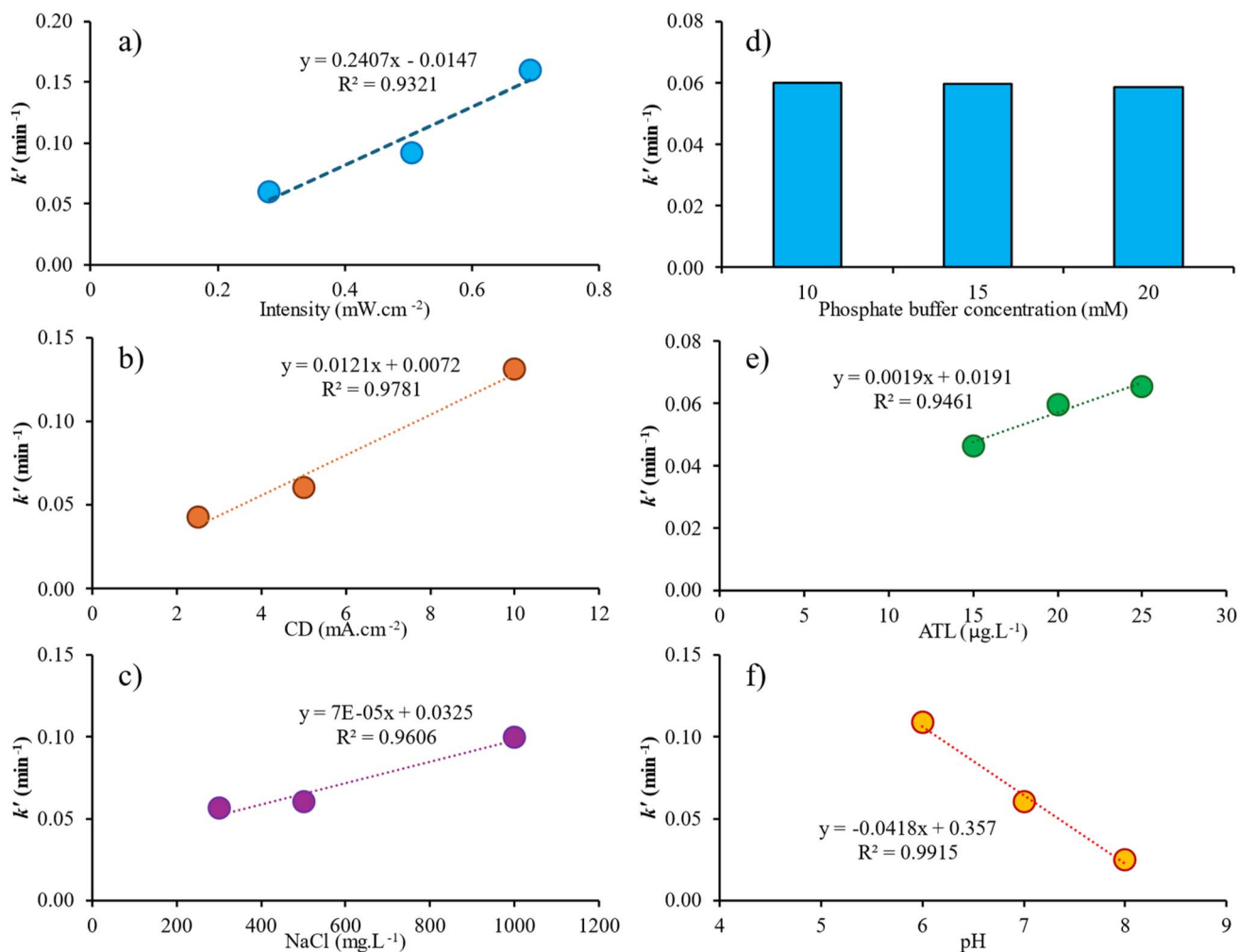
Fig. 2 ATL removal using the UV/EO process under various UV intensities (a), CDs (b), NaCl concentrations (c), phosphate buffer concentrations (d), ATL concentrations (e), and pH values (f).

concentrations of 300, 500, and 1000 mg L^{-1} were 0.0560, 0.0599, and 0.0995 min^{-1}, respectively (SI Fig. 7). The k' value at the initial NaCl concentration of 1000 mg L^{-1} was nearly twice that observed at 300 and 500 mg L^{-1}. The chloride ion (Cl$^-$) is a substrate for anodic oxidation and photochemical pathways to produce FAC, which is further photolyzed to form $\cdot$OH and RCS (eqn (2)–(5)). The k' value can be estimated by eqn (12). At low NaCl concentrations (300–500 mg L^{-1} or 5.13–8.56 mM Cl$^-$), ATL removal was dominated by $\cdot$OH, resulting in a slight increase in k'. The minor effect of RCS on ATL removal was revealed and is discussed in Section 3.2.7. High concentrations of NaCl (1000 mg L^{-1} or 17.12 mM Cl$^-$) increased the solution conductivity and reduced ohmic loss, which increased the current efficiency for anodic water oxidation. Higher conductivity could facilitate more efficient electron transfer, allowing greater anodic generation of $\cdot$OH through direct oxidation of water and subsequent indirect oxidation in the bulk.[55,56] Thus, NaCl addition could nonlinearly enhance formation of $\cdot$OH on the surface and in the bulk, promoting a significant increase in the k' value. Additionally, elevated NaCl concentrations

increased the formation of free chlorine (35 mg L^{-1}), which could subsequently react with ATL.

$$k' \approx k_{\cdot OH}[\cdot OH] + k_{Cl\cdot}[Cl\cdot] + k_{FAC}[FAC] + kUV[\Phi I] \quad (12)$$

3.2.4. Phosphate buffer concentration. To understand the effect of electric potential, various phosphate buffer concentrations were used to modify the system's conductivity. The system was subjected to different electric potentials while maintaining a constant CD (5 mA cm^{-2}). To ensure a stable current across varying electric potentials, phosphate buffer concentrations were adjusted to 10, 15, and 20 mM; these buffer concentrations induced current potentials of 7.90, 8.24 and 9.60 V, respectively. However, the removal efficiencies of ATL remained consistent, with approximately 91% removal achieved within 30 min (Fig. 2d), suggesting that the current potential had no significant impact on the removal of ATL. In addition, the ATL was removed by either chlorine reaction or anodic oxidation, while a direct electron transfer from the electrode surface was minor. Although the experiment was conducted

with various electric potentials, the k' values remained relatively stable, ranging from 0.0588 to 0.0599 min^{-1} (SI Fig. 8).

3.2.5. ATL concentration. The UV/EO process effectively removed ATL concentrations of 15, 20 and 25 μg L^{-1} to non-detectable levels within 40, 50, and 50 min, respectively (Fig. 2e). The highest k' value was observed at an initial ATL concentration of 15 μg L^{-1}, with a value of 0.0655 min^{-1} (SI Fig. 9). The k' values for initial ATL concentrations of 20 and 25 μg L^{-1} were 0.0599 and 0.0464 min^{-1}, respectively. The results revealed an inverse relationship between the initial ATL concentration and the k' value. This suggested that as the initial concentration of ATL decreased, the rate of its degradation (as indicated by k') was more rapid. A possible explanation could be that lower concentrations of ATL led to less competition for reactive species or a more efficient reaction environment, resulting in an enhanced rate of degradation. In addition, the ATL degradation products may either inhibit the reaction or require additional energy to degrade, thereby affecting the overall kinetics. The transformation of amine moieties in ATL during UV/chlorine treatment involved complex mechanisms influenced by reactant concentrations.[57] Similar findings were reported in previous studies, wherein a decrease in substrate concentrations accelerated the reaction rate due to more favorable conditions.[58,59]

3.2.6. pH. The UV/EO process exhibited the highest efficiency for ATL removal at pH 6, followed by pH 7 and pH 8 (Fig. 2f). Consequently, complete degradation of ATL was achieved most rapidly at pH 6, with total removal occurring within 25 min. At pH 7, ATL concentrations fell below detectable levels within 50 min. In contrast, the removal rate was lowest at pH 8, where ATL was no longer detected after 100 min. The change in pH affected free chlorine species. The [OCl$^-$]/[HOCl] ratio increased with higher pH values.[14,60] The oxidation potentials of HOCl and OCl$^-$ were 1.49 and 0.90 V,[44,61] respectively, implying that HOCl was more reactive towards organic compounds than OCl$^-$. In addition, oxygen evolution preferentially occurred under acidic conditions, leading to longer lifetimes of 'OH.[62] On the other hand, several substances in alkaline solution (hydroxide, carbonate, bicarbonate) could act as scavengers of 'OH,[63] reducing the rate of ATL removal. The k' values for pH 6, pH 7, and pH 8 were 0.1084, 0.0599, and 0.0248 min^{-1}, respectively (SI Fig. 10). The enhanced ATL removal at pH 6 could be attributed to two factors. Firstly, the dominance of HOCl under low pH conditions facilitated the generation of 'OH.[38,64] Among reactive oxygen species, 'OH is primarily formed at pH levels below 7.5 by UV photolysis of HOCl, while O$^{•-}$ is produced via the photolysis of OCl$^-$ at higher pH values (eqn (5)).[38] Since 'OH exhibited a higher oxidation potential (2.80 V) than O$^{•-}$ (2.42 V), a higher removal efficiency of recalcitrant compounds could be expected.[56] Secondly, the reaction rate of OCl$^-$ with 'OH was approximately four times faster than that of HOCl, with reported rate constants of 8.8×10^9 and 2×10^9 M^{-1} s^{-1}, respectively.[65] Thus, the higher fraction of OCl$^-$ could substantially inhibit the 'OH oxidation. As a result, increasing the pH from pH 6 to pH 7 and pH 8 led to a reduction in the removal rate by 45% and 77%, respectively.

3.2.7. Free radicals. The ATL removal was reduced when scavengers (i.e., pCBA and BA) were added. At 60 min, 90% and 87% of the ATL were removed after adding pCBA and BA, respectively (Fig. 3). Although the amounts of ATL removed from samples containing pCBA and BA were comparable to those in the non-scavenger samples, the presence of pCBA and BA reduced the overall degradation rate. The k' values for the non-scavenger sample and the samples with pCBA and BA additions were 0.0599, 0.0367, and 0.0329 min^{-1}, respectively. The k' value for the pCBA sample decreased significantly, by 39%, indicating that 'OH played a dominant role in ATL oxidation. The further reduction in k' values with BA suggested that RCS also participated in ATL degradation, albeit to a lesser extent than 'OH. The k' value for the BA sample decreased by 45%, compared to the non-scavenger sample. Cl' could rapidly react with chloride ions to form Cl$_2^{•-}$ at a rate that limited their steady-state concentrations ($k_1 = 6.5 \times 10^9$ M^{-1} s^{-1}), while the reverse reaction occurred more slowly (Cl$_2^{•-}$ ↓ Cl' + Cl$^-$; $k_2 = 1.1 \times 10^5$ M^{-1} s^{-1}). In comparison, the reaction of 'OH with chloride ions proceeded at a lower rate ($k_3 = 4.3 \times 10^9$ M^{-1} s^{-1}).[46] A previous study reported that the major free radical to react with ATL was 'OH, rather than RCS.[66] 'OH can react at the aromatic ring or the secondary amine of ATL with rate constants ($k_{•OH}$) of 4.8–7.19 × 10^9 M^{-1} s^{-1}.[29,67,68]

To quantify the concentration of free radicals, the removal rates of pCBA and BA were determined. The k' values for pCBA and BA removal were 0.0220 and 0.0286 min^{-1}, respectively. The amount of 'OH and RCS formed in the system was calculated as described in SI Text 1. The amount of 'OH and RCS formed in the system was 7.33×10^{-14} M and 2.44×10^{-15} M, respectively. These active radicals contributed to a $k_{Cl•}$ of 1.55×10^{11} M^{-1} s^{-1}, implying that ATL was more sensitive to Cl' than 'OH. The calculation of $k_{Cl•}$ is described in SI Text 2. However, the generation of 'OH was approximately 30 times greater than that of Cl'; thus, 'OH was the major oxidant in the ATL degradation.

3.3. Correlation between specific energy consumption and k' value

One of the primary constraints in the implementation of the UV/EO process is the operational cost, which is predominantly
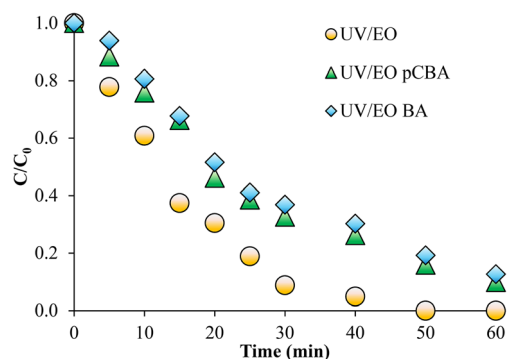

Fig. 3 ATL degradation by the UV/EO process in the presence of scavengers (BA and pCBA) (BA/pCBA 1 mM, ATL 20 μg L^{-1}, pH 7, NaCl 500 mg L^{-1}, 1 UV lamp, $n = 1$).

attributed to energy consumption. The specific energy consumption was calculated based on 90% ATL removal. The energy consumption at a fixed CD of 5 mA cm^{-2} exhibited a strong linear relationship with the inverse of the k' value (Fig. 4). As k' increased, the energy consumption decreased significantly. The data showed a high correlation ($R^2 = 1.000$), with the regression equation given as $E = 0.1352 (1/k') + 0.0042$. This linear line suggests that energy consumption decreases proportionally with increasing reaction kinetics. The trend revealed that a factor modification to enhance the electrochemical activity (higher k') could enhance mass transfer and minimize energy demand in the UV/EO process.[44,69,70] In addition, the elevated k' enabled a more compact system because of the reduced time requirement. On the other hand, an increase in CD to 10 mA cm^{-2} resulted in greater energy consumption, although k' also increased. A previous study also reported that the energy demand increased with higher CD.[71] This observation indicated that the primary energy demand in the UV/EO process was the electrical current applied to the electrodes.

3.4. Toxicity

The bacterial toxicity levels of the samples treated with the UV/EO process at 0, 30, 60, 120, and 180 min were 10%, 17%, 17%, 19%, and 13%, respectively (Fig. 5). Interestingly, the bacterial growth inhibition nearly doubled within the first 120 minutes before subsequently declining. This raised an awareness of the formation of highly toxic compounds during the oxidation of ATL. The ATL degradation pathway during the UV/EO process was expected to be similar to that reported in the previous study on the UV/chlorine process. In these pathways, ATL is degraded through hydroxylation and chlorination of the aromatic ring, cleavage of the ether bond, and oxidation of the amine moiety.[30] In addition, variation in toxicity levels may result from a synergistic effect of ˙OH and RCS, which can react with ATL to form disinfection by-products (DBPs), such as trihalomethanes (THMs) and halo-acetaldehydes (HALs). Furthermore, the amine moiety in the atenolol structure can lead to the formation of nitrogenous DBPs.[30,66] In addition, ˙OH oxidation can render substances more reactive towards chlorine and RCS.[30,72,73] RCS and FAC can react with ATL to form halonitromethanes (HNMs) and
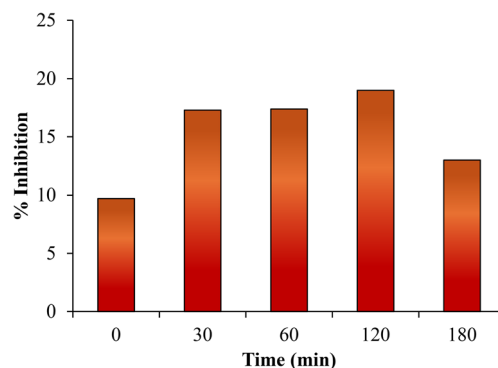

Fig. 5 Inhibition of bacterial growth in water treated using the UV/EO process.

haloacetonitriles (HANs), with high genotoxicity and cytotoxicity, rather than carbonaceous DBPs.[30,74,75] These intermediate products may exhibit higher toxicity levels than the parent compound (ATL). The formation of intermediates with higher toxicity aligned with findings from similar studies on β-blockers that were conducted under the UV/chlorine treatment regime.[57,76] A toxicity assessment using the bioluminescent freshwater bacterium (*i.e.*, *Aliivibrio fischeri*) revealed that intermediates formed during the ATL oxidation exhibited higher toxicity than the parent compound.[30] However, extending the treatment time to over 120 min resulted in a reduction in bacterial inhibition, suggesting a progressive degradation of toxic intermediates into less harmful byproducts. These findings highlight the necessity for a comprehensive toxicity evaluation of intermediates and demonstrate that optimization of the UV/EO reaction time is required to minimize the formation of toxic transformation products while ensuring effective pollutant removal.

4. Conclusion

The highest ATL removal was observed in the UV/EO process, followed by UV/chlorine, EO, chlorination, and UV irradiation. The UV/EO process exhibited a synergistic effect on the ATL removal. The efficiency of the UV/EO process for the removal of ATL depended directly on the UV intensity, NaCl concentration, and CD. On the other hand, increases in pH and the initial ATL concentration exhibited an inverse effect, leading to a reduction in removal efficiency. Variations in current potential had no impact on the ATL removal. The energy consumption of the UV/EO process exhibited an inverse proportionality to the k' value. Although ˙OH and RCS contributed to the degradation of ATL, ˙OH played the major role, rather than RCS. The kinetic degradation of ATL by ˙Cl ($k_{Cl·}$) was 1.55×10^{11} M^{-1} s^{-1}. The intermediate products formed during the UV/EO treatment for 120 min exhibited higher toxicity levels than the parent compound (ATL). Extending the treatment time beyond 120 min decreased the bacterial inhibition.

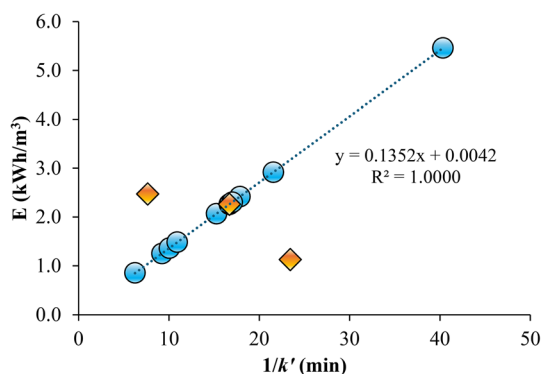## Conflicts of interest

There are no conflicts to declare.

Fig. 4 Correlation between specific energy consumption and $1/k'$ (circles = fixed CD at 5 mA cm^{-2}, diamonds = CD values of 2.5, 5, and 10 mA cm^{-2}).

Data availability

Additional data are available on request.

The authors declare that the data supporting the findings of this study are available within the paper and its SI. Supplementary information is available. See DOI: https://doi.org/10.1039/d5ra05011a.

Acknowledgements

References

1 N. Vieno, H. Härkki, T. Tuhkanen and L. Kronberg, Occurrence of pharmaceuticals in river water and their elimination in a pilot-scale drinking water treatment plant, *Environ. Sci. Technol.*, 2007, 5077–5084.

2 R. Rezaei, A. A. Aghapour, R. A. Chavshin and R. Bargeshadi, Biodegradation of the atenolol and nitrogen removal using the sequencing, *Bioresour. Technol. Rep.*, 2022, 101109.

3 A. Mohseni-Bandpei, S. Ghasemi, A. Eslami, M. Rafiee, M. Sadani and F. Ghanbari, Degradation of atenolol by CuFe2O4/visible light/oxidant: effects of electron acceptors, synergistic effects, degradation pathways, and mechanism", *J. Photochem. Photobiol., A*, 2021, **418**, 113425.

4 B. Ramasamy, J. Jeyadharmarajan and P. Chinnaiyan, Novel organic assisted Ag-ZnO photocatalyst for atenolol and acetaminophen photocatalytic degradation under visible radiation: performance and reaction mechanism, *Environ. Sci. Pollut. Res.*, 2021, **28**, 39637–39647.

5 M. Maurer, B. Escher, R. Richle, C. Schaffne and A. Alder, Elimination of β-blockers in sewage treatment plants, *Water Res.*, 2007, 1614–1622.

6 M. DellaGreca, R. M. Iesce, P. Pistillo, L. Previtera and F. Temussi, Unusual products of the aqueous chlorination of atenolol, *Chemosphere*, 2009, 730–734.

7 Y. Yang, X. Zhang, J. Jiang, J. Han, W. Li, X. Li, K. Leung, S. Snyder and P. Alvarez, Which micropollutants in water environments deserve more attention globally?, *Environ. Sci. Technol.*, 2022, **56**(1), 13–29.

8 J. Quintana, R. Rodil and R. Cela, Reaction of β-blockers and β-agonist pharmaceuticals with aqueous chlorine. Investigation of kinetics and by-products by liquid chromatography quadrupole time-of-flight mass spectrometry, *Anal. Bioanal. Chem.*, 2012, **403**, 2385–2395.

9 X. Liu, T. Zhang, Y. Zhou, L. Fang and Y. Shao, Degradation of atenolol by UV/peroxymonosulfate: kinetics, effect of operational parameters and mechanism, *Chemosphere*, 2013, **93**(11), 2717–2724.

10 B. Özyurt and Ş. Camcıoğlu, Applications of Combined Electrocoagulation and Electrooxidation Treatment to Industrial Wastewaters, *Wastewater and Water Quality*, InTech, 2018, DOI: 10.5772/intechopen.75460.

11 X. Kong, Z. Wu, Z. Ren, K. Guo, S. Hou, Z. Hua, X. Li and J. Fang, Degradation of lipid regulators by the UV/chlorine process: Radical mechanisms, chlorine oxide radical (ClO·)-mediated transformation pathways and toxicity changes, *Water Res.*, 2018, 242–250.

12 P. Otter, K. Mette, R. Wesch, T. Gerhardt, F.-M. Krüger, A. Goldmaier, F. Benz, P. Malakar and T. Grischek, Oxidation of Selected Trace Organic Compounds through the Combination of Inline Electro-Chlorination with UV Radiation (UV/ECl2) as Alternative AOP for Decentralized Drinking Water Treatment, *Water*, 2020, 3275.

13 G. Khajouei, H. Finklea and L.-S. Lin, UV/chlorine advanced oxidation processes for degradation of contaminants in water and wastewater: a comprehensive review, *J. Environ. Chem. Eng.*, 2022, **10**, 107508.

14 N. Kishimoto, Y. Katayama, M. Kato and H. Otsu, Technical feasibility of UV/electro-chlorine advanced oxidation process and pH response, *Chem. Eng. J.*, 2018, **334**, 2363–2372.

15 J. Uwayezu, I. Carabante, P. van Hees, P. Karlsson and J. Kumpiene, Combining electrochemistry and ultraviolet radiation for the degradation of per- and poly-fluoroalkyl substances in contaminated groundwater and wastewater, *J. Water Process Eng.*, 2023, **54**, 104028.

16 Z. Heidari, R. Pelalak and M. Zhou, A critical review on the recent progress in application of electro-Fenton process for decontamination of wastewater at near-neutral pH, *Chem. Eng. J.*, 2023, **474**, 145741.

17 Y. Lin, J. Qiao, Y. Sun and H. Dong, The profound review of Fenton process: What's the next step?, *J. Environ. Sci.*, 2025, **147**, 114–130.

18 G. Kamble and Y.-C. Ling, Solvothermal synthesis of facet-dependent BiVO4 photocatalyst with enhanced visible-light-driven photocatalytic degradation of organic pollutant: assessment of toxicity by zebrafish embryo, *Sci. Rep.*, 2020, **10**, 12993.

19 R. Ghaware, N. Birajdar, G. Kamble and S. Kolekar, Degradation of organic Pollutant by Using of BiVO4–NiFe2O4 Heterostructure Photocatalyst under Visible Light Irradiation: Assessment of Detoxicity Study Using Cirrhinus mrigala, *Langmuir*, 2024, **40**(28), 14426–14439.

20 Y. Lee and U. von Gunten, Oxidative transformation of micropollutants during municipal wastewater treatment: Comparison of kinetic aspects of selective (chlorine, chlorine dioxide, ferrateVI, and ozone) and non-selective oxidants (hydroxyl radical), *Water Res.*, 2010, 555–566.

21 J. Jin, M. G. El-Din and J. R. Bolton, Assessment of the UV/Chlorine process as an advanced oxidation process, *Water Res.*, 2011, **45**(4), 1890–1896.

22 Z. Lang, X. Song, G. Song, L. Han, Q. Zhang and M. Zhou, A flow-through UV/electro-chlorine process for cost-effective and multifunctional purification of marine aquaculture wastewater, *Environ. Chem. Eng.*, 2022, 107262.

23 M. Ren, S. Sun, S. Wu, Y. Shi, Z.-j. Wang, H. Cao and Y. Xie, The structure-activity relationship of aromatic compounds in advanced oxidation processes:a review, *Chemosphere*, 2022, 134071.

24 Z. Wu, J. Fang, Y. Xiang, C. Shang, X. Li, F. Meng and X. Yang, Water Research, *Roles of Reactive Chlorine Species*

in *Trimethoprim Degradation in the UV/chlorine Process: Kinetics and Transformation Pathways*, 2016, pp. 272–282.

25 D. Minakata, D. Kamath and S. Maetzold, Mechanistic insight into the reactivity of chlorine-derived radicals in the aqueous-phase UV-chlorine advanced oxidation process: Quantum mechanical calculations, *Environ. Sci. Technol.*, 2017, **51**(12), 6918–6926.

26 Y. Lei, X. Lei, P. Westerhoff, X. Zhang and X. Yang, Reactivity of chlorine radicals (Cl$^•$ and Cl$_2^{•−}$) with dissolved organic matter and the formation of chlorinated byproducts, *Environ. Sci. Technol.*, 2021, **55**(1), 689–699.

27 X.-F. Li and W. Mitch, Drinking water disinfection byproducts (DBPs) and human health effects: Multidisciplinary challenges and opportunities, *Environ. Sci. Technol.*, 2018, **52**, 1681–1689.

28 X. Liu and Z. He, Decreased formation of disinfection by-products during electrochemical leachate oxidation and their post-removal by electro-adsorption, *Sci. Total Environ.*, 2020, **730**, 139171.

29 B. Wols, D. Harmsen, E. Beerendonk and C. Hofman-Caris, Predicting pharmaceutical degradation by UV (LP)/H2O2 processes: a kinetic model, *Chem. Eng. J.*, 2014, **255**, 334–343.

30 Y.-Q. Gao, N.-Y. Gao, J.-X. Chen, J. Zhang and D.-Q. Yin, Oxidation of β-blocker atenolol by a combination of UV light and chlorine: kinetics, degradation pathways and toxicity assessment, *Sep. Purif. Technol.*, 2020, **231**, 115927.

31 E. Brillas and C. Martínez-Huitle, Decontamination of wastewaters containing synthetic organic dyes by electrochemical methods. an updated review, *Appl. Catal., B*, 2015, **166–167**, 603–643.

32 H. Barzoki, A. Dargahi, A. Shabanloo, A. Ansari and S. Bairami, Electrochemical advanced oxidation of 2,4-D herbicide and real pesticide wastewater with an integrated anodic oxidation/heterogeneous electro-Fenton process, *J. Water Process Eng.*, 2023, **56**, 104429.

33 R. O. Rahn, M. I. Stefan, J. R. Bolton, E. Goren, P.-S. Shaw and K. R. Lykke, Quantum yield of the iodide-iodate chemical actinometer: dependence on wavelength and concentrations, *Photochem. Photobiol.*, 2003, 146–152.

34 J. Bolton, M. Stefan, P.-S. Shaw and K. Lykke, Determination of the quantum yields of the potassium ferrioxalate and potassium iodide–iodate actinometers and a method for the calibration of radiometer detectors, *J. Photochem. Photobiol., A*, 2011, **222**(1), 166–169.

35 N. Hoang, V. Nguyen, N. Tuan, T. Manh, P.-C. Le, D. Tac and F. Mwazighe, Degradation of dyes by UV/persulfate and comparison with other UV-based advanced oxidation processes: kinetics and role of radicals, *Chemosphere*, 2022, **298**, 134197.

36 M. Kwon, Y. Yoon, S. Kim, Y. Jung, T. Hwang and J. Kang, Removal of sulfamethoxazole, ibuprofen and nitrobenzene by UV and UV/chlorine processes: a comparative evaluation of 275 nm LED-UV and 254 nm LP-UV, *Sci. Total Environ.*, 2018, **637–638**, 1351–1357.

37 V. Pereira, H. Weinberg, K. Linden and P. Singer, UV Degradation Kinetics and Modeling of Pharmaceutical Compounds in Laboratory Grade and Surface Water *via* Direct and Indirect Photolysis at 254 nm, *Environ. Sci. Technol.*, 2007, **41**(5), 1682–1688.

38 J. Fang, Y. Fu and C. Shang, The roles of reactive species in micropollutant degradation in the UV/Free chlorine system, *Environ. Sci. Technol.*, 2014, **48**, 1859–1868.

39 W.-L. Wang, Q.-Y. Wu, N. Huang, T. Wang and H.-Y. Hu, Synergistic effect between UV and chlorine (UV/chlorine) on the degradation of carbamazepine: influence factors and radical species, *Water Res.*, 2016, **98**, 190–198.

40 E. Rosenfeldt, K. Linden, S. Canonica and U. von Gunten, Comparison of the efficiency of $^•$OH radical formation during ozonation and the advanced oxidation processes O$_3$/H$_2$O$_2$ and UV/H$_2$O$_2$, *Water Res.*, 2006, **40**(20), 3695–3704.

41 Q. Qiao, S. Singh, S.-L. Lo, J. Jin, Y. Yu and L. Wang, Effect of current density and pH on the electrochemically generated active chloro species for the rapid mineralization of p-substituted phenol, *Chemosphere*, 2021, **275**, 129848.

42 A. dos Santos, H. Shen, M. Lanza, Q. Li and S. Garcia-Segura, Electrochemical oxidation of surfactants as an essential step to enable greywater reuse, *Environ. Technol. Innovation*, 2024, **34**, 103563.

43 H. Brouwer, Testing for Chemical Toxicity Using Bacteria: an undergraduate laboratory experiment, *Chem. Educ.*, 1991, **68**(8), 695.

44 F. Moreira, R. Boaventura, E. Brillas and V. Vilar, Electrochemical advanced oxidation processes: a review on their application ot synthetic and real wastewaters, *Appl. Catal., B*, 2017, **202**, 217–261.

45 X. Liu, L. Fang, Y. Zhou, T. Zhang and Y. Shao, Comparison of UV/PDS and UV/H$_2$O$_2$ processes for the degradation of atenolol in water, *J. Environ. Sci.*, 2013, **25**(8), 1519–1528.

46 J. Wang and S. Wang, Reactive species in advanced oxidation processes: formation, identification and reaction mechanism, *Chem. Eng. J.*, 2020, **401**, 126158.

47 C. Wang, M.-C. Xiong, X. Zhao and K.-H. Liu, Kinetics study on reaction of atenolol with singlet oxygen by directly monitoring the $^1O_2$ phosphorescence, *Chin. J. Chem. Phys.*, 2021, **34**, 406–412.

48 M. O'Connor, S. Helal, D. Latch and W. Arnold, Quantifying photo-production of triplet excited states and singlet oxygen from effluent organic matter, *Water Res.*, 2019, **156**, 23–33.

49 M. Dong, R. Trenholm and F. Rosario-Ortiz, Photochemical degradation of atenolol, carbamazepine, meprobamate, phenytoin and primidone in wastewater effluents, *J. Hazard. Mater.*, 2015, **282**, 216–223.

50 K. Cheng, L. Zhang and G. McKay, Evaluating the microheterogeneous distribution of photochemically generated singlet oxygen using furfuryl amine, *Environ. Sci. Technol.*, 2023, **57**(19), 7568–7577.

51 J. Li, S. Zhou, M. Li, E. Du and X. Liu, Mechanism insight of acetaminophen degradtion by the UV/chlorine process: kinetics, intermediates, and toxicity assessment, *Environ. Sci. Pollut. Res.*, 2019, **26**(24), 25012–25025.

52 P. Boontham and S. Phattarapattamawong, Influencing factors on performance of electro-oxidation and UV/electro-oxidation for removal of atrazine: kinetics, long-term stability and toxicity, *Chemosphere*, 2025, **374**, 144187.

53 S. Periyasamy and M. Muthuchamy, Electrochemical degradation of psychoactive drug caffeine in aqueous solution using graphite electrode, *Environ. Technol.*, 2018, **39**(18), 2373–2381.

54 R. Flores-Terreros, E. Serna-Galvis, J. Navarro-Laboulais, R. Torres-Palma and J. Nieto-Juarez, An alternative approach to the kinetic modeling of pharmaceuticals degradation in high saline water by electrogenerated active chlorine species, *J. Environ. Manage.*, 2022, **315**, 115119.

55 S. Sundarapandiyan, T. Renitha, J. Sridevi, B. Chandrasekaran, P. Saravanan and G. Raju, Mechanistic insight into active chlorine species mediated electrochemical degradation of recalcitrant phenolic polymers, *RSC Adv.*, 2014, **4**, 59821–59830.

56 X. Wang and L. Zhang, Kinetic study of hydroxyl radical formation in a continuous hydroxyl generation system, *RSC Adv.*, 2018, **8**, 40632–40638.

57 J. Ra, H. Yoom, H. Son, T.-M. Hwang and Y. Lee, Transformation of an amine moiety of atenolol during water treatment with Chlorine/UV: reaction kinetics, products, and mechanisms, *Environ. Sci. Technol.*, 2019, **53**(13), 7653–7662.

58 M. Bansal, A. Singh and S. Kumar, Effect of substrate concentration on the reaction kinetics of degradation processes, *Environ. Sci. Technol.*, 2013, **47**(15), 8495–8502.

59 J. Smith, M. Davis and R. Hall, Kinetic analysis of reaction rates in the degradation of organic contaminants, *J. Hazard. Mater.*, 2017, **336**, 100–108.

60 K. Hansen, S. Willach, M. Antoniou, H. Mosbæk, H.-J. Albrechtsen and H. Andersen, Effect of pH on the formation of disinfection byproducts in swimming pool water – Is less THM better?, *Water Res.*, 2012, **46**(19), 6399–6409.

61 S. van Haute, B. Zhou, Y. Luo, I. Sampers, M. Vanhaverbeke and P. Millner, The use of redox potential to estimate free chlorine in fresh produce washing operations: Possibilities and limitations, *Postharvest Biol. Technol.*, 2019, **156**, 110957.

62 J. Zambrano, H. Park and B. Min, Enhancing electrochemical degradation of phenol at optimum pH condition with a Pt/Ti anode electrode, *Environ. Technol.*, 2020, **41**(24), 3248–3259.

63 T. Enache, A. Chiorcea-Paquim, O. Fatibello-Filho and A. Oliveira-Brett, Hydroxyl radicals electrochemically generated *in situ* on a boron-doped diamond electrode, *Electrochem. Commun.*, 2009, **11**(7), 1342–1345.

64 C. Trellu, H. Vargas, E. Mousset, N. Oturan and M. Oturan, Electrochemical technologies for the treatment of pesticides, *Curr. Opin. Electrochem.*, 2021, **26**, 100677.

65 X. Kong, J. Jiang, J. Ma, Y. Yang, W. Liu and Y. Liu, Degradation of atrazine by UV/chlorine: efficiency, influencing factors, and products, *Water Res.*, 2016, **90**, 15–23.

66 Y. Yeom, J. Han, X. Zhang, C. Shang, T. Zhang, X. Li, X. Duan and D. Dionysiou, A review on the degradation efficiency, DBP formation, and toxicity variation in the UV/chlorine treatment of micropollutants, *Chem. Eng. J.*, 2021, **42**, 130053.

67 K. Kovács, T. Tóth and L. Wojnárovits, Evaluation of advanced oxidation processes for β-blockers degradation: a review, *Water Sci. Technol.*, 2022, **85**(2), 685–705.

68 K. Kovács, A. Simon, T. Tóth and L. Wojnárovits, Free radical chemistry of atenolol and propranolol investigated by pulse and gamma radiolysis, *Radiat. Phys. Chem.*, 2022, **196**, 110141.

69 S. Ganiyu, C. Martínez-Huitle and M. Oturan, Electrochemical advanced oxidation processes for wastewater treatment: advances in formation and detection of reactive species and mechanisms, *Curr. Opin. Electrochem.*, 2021, **27**, 100678.

70 G. Vieira, I. Segundo, J. Santos, A. Gondim, E. dos Santos and C. Martinez-Huitle, Electro-oxidation of wastewater from a beauty salon: the influence of electrolyte type in the removal of organic load and energy consumption, *Process Saf. Environ. Prot.*, 2023, **177**, 1260–1271.

71 A. Rodrigues, F. Souiad, A. Fernandes, A. Baia, M. Pacheco, L. Ciriaco, Y. Bendaoud-Boulahlib and A. Lopes, Treatment of fruit processing wastewater by electrochemical and activated persulfate processes: toxicological and energetic evaluation, *Environ. Res.*, 2022, **209**, 112868.

72 C. Wang, Z. Ying, M. Ma, M. Huo and W. Yang, Degradation of micropollutants by UV-Chlorine treatment in reclaimed water: pH effects, formation of disinfectant byproducts, and toxicity assay, *Water*, 2019, **11**(12), 2639.

73 X. Ruan, Y. Xiang, C. Shang, S. Cheng, J. Liu, Z. Hao and X. Yang, Molecular characterization of transformation and halogenation of natural organic matter during the UV/chlorine AOP using FT-ICR mass spectrometry, *J. Environ. Sci.*, 2021, **102**, 24–36.

74 E. Wagner and M. Plewa, CHO cell cytotoxicity and genotoxicity analyses of disinfection by-products: an updated review, *J. Environ. Sci.*, 2017, **58**, 64–75.

75 X. Wei, M. Yang, Q. Zhu, E. Wagner and P. Plewa, Comparative quantitative toxicology and QSAR modeling of the haloacetonitriles: forcing agents of water disinfection byproduct toxicity, *Environ. Sci. Technol.*, 2020, **54**(14), 8909–8918.

76 R. Xiong, Z. Lu, Q. Tang, X. Huang, H. Ruan, W. Jiang, Y. Chen, Z. Liu, J. Kang and D. Liu, UV-LED/chlorine degradation of propranolol in water: degradation pathway and product toxicity, *Chemosphere*, 2020, **248**, 125957.